British Journal of Pharmacology (2007) 152, 1260–1271
 0007–1188/07 $30.00
www.brjpharmacol.org

RESEARCH PAPER

Analysis of the pharmacokinetic/pharmacodynamic relationship of a small molecule CXCR3 antagonist, NBI-74330, using a murine CXCR3 internalization assay

LA Jopling[1], GF Watt[1], S Fisher[2], H Birch[3], S Coggon[3] and MI Christie[1]

[1]*Department of Pharmacology, UCB Inflammation Discovery, Granta Park, Great Abington, Cambridgeshire, UK;* [2]*Department of Molecular and Cellular Systems, UCB Inflammation Discovery, Granta Park, Great Abington, Cambridgeshire, UK and* [3]*Department of Drug Metabolism and Pharmacokinetics, UCB Inflammation Discovery, Granta Park, Great Abington, Cambridgeshire, UK*

Background and purpose: Pharmacokinetic/pharmacodynamic (PK/PD) models are necessary to relate the degree of drug exposure *in vivo* to target blockade and pharmacological efficacy. This manuscript describes a murine agonist-induced CXCR3 receptor internalization assay and demonstrates its utility for PK/PD analyses.
Experimental approach: Activated murine DO11.10 cells were incubated with agonist in the presence or absence of a CXCR3 antagonist and changes in surface CXCR3 expression were detected by flow cytometry. For PK/PD analysis, mice were dosed with a small molecule CXCR3 antagonist, NBI-74330, (100 mg kg^{-1}) orally or subcutaneously and plasma samples taken at specified timepoints for the CXCR3 internalization assay.
Key results: Surface CXCR3 expression was specifically decreased in response to CXCL9, CXCL10 and CXCL11. CXCL11 was the most potent CXCR3 agonist in buffer ($pA_{50} = 9.23 \pm 0.26$) and the pA_{50} for CXCL11 was unaltered in murine plasma ($pA_{50} = 9.17 \pm 0.15$). The affinity of a small molecule CXCR3 antagonist, NBI-74330, was obtained in the absence or presence of plasma (buffer pA_2 value: 7.84 ± 0.14; plasma pK_B value 6.36 ± 0.01). Administration of NBI-74330 to mice resulted in the formation of an N-oxide metabolite, also an antagonist of CXCR3. Both antagonists were detectable up to 7 h post oral dose and 24 h post subcutaneous dose. Measurement of CXCR3 internalization demonstrated significant antagonism of this response *ex vivo*, 24 h following subcutaneous administration of NBI-74330.
Conclusions and implications: The CXCR3 receptor internalization assay provides a robust method for determining agonist potency orders, antagonist affinity estimates and PK/PD analyses, which discriminate between dosing regimens for the CXCR3 antagonist NBI-74330.
British Journal of Pharmacology (2007) **152,** 1260–1271; doi:10.1038/sj.bjp.0707519; published online 5 November 2007

Keywords: CXCR3; CXCL9; CXCL10; CXCL11; receptor internalization; NBI-74330; pharmacokinetic/pharmacodynamic

Abbreviations: E/[A], agonist concentration effect curve; PD, pharmacodynamic; PK, pharmacokinetic

Introduction

The drug discovery process requires appropriate pharmacokinetic/pharmacodynamic (PK/PD) models to understand the relationship between drug exposure and pharmacological effect. PK/PD models help facilitate the transition of molecules from research to development and onto the market by minimizing drug attrition due to poor PK parameters (Walker, 2004). PK/PD models provide vital information such as the mode of action of a molecular target, dose range and regimen, therapeutic window of a drug and may also enable biomarker identification (Colburn, 2000). Tolerance of blood or plasma within an appropriate assay system assists with the development of PK/PD modelling and may provide information on the properties required of a potential drug candidate (Walker, 2004).

Approximately 27% of current Food and Drug Administration-approved drugs target the G-protein-coupled receptor (GPCR) family (Overington *et al*., 2006) to which chemokine receptors belong. The chemokine receptor subfamily provides a number of attractive drug targets. Chemokines and chemokine receptors have been implicated in a variety of inflammatory conditions and a role for CXCR3 has

Correspondence: Dr LA Jopling, Department of Pharmacology, UCB Inflammation Discovery, Granta Park, Great Abington, Cambridgeshire CB21 6GS, UK.
E-mail: louise.jopling@ucb-group.com
Received 20 July 2007; revised 17 September 2007; accepted 21 September 2007; published online 5 November 2007

been suggested in disorders such as rheumatoid arthritis, multiple sclerosis and transplant rejection based on receptor and/or agonist expression profiles within clinical samples or from murine models of disease (Sorensen *et al*., 1999; Hancock *et al*., 2000; Eriksson *et al*., 2003; Pease and Williams, 2006).

The human CXCR3 receptor was originally identified and cloned in the mid-1990s (Marchese *et al*., 1995; Loetscher *et al*., 1996) and while CXCR3 mRNA has been detected in monocytes, neutrophils and mast cells, the T cell is the predominant cell type that expresses this receptor (Loetscher *et al*., 1996). Chemokine receptor expression profiles on polarized human T cells demonstrated CXCR3 to be strongly associated with the development of $CD4^+$ Th1 cells (Bonecchi *et al*., 1998; Sallusto *et al*., 1998). Cellular activation through CXCR3 occurs in response to binding of the agonists, CXCL9, CXCL10 or CXCL11 (Rabin *et al*., 1999; Tensen *et al*., 1999), which are produced in response to IFN-γ, implicating the CXCR3-receptor activation axis in Th1-dominated diseases.

Human CXCR3 receptor function has been extensively studied using a range of assay systems such as radioligand binding, intracellular calcium flux, *in vitro* migration or receptor internalization assays. CXCL11 and CXCL10 are the most widely studied CXCR3 ligands and the data suggest that CXCL11 is the most efficacious agonist for the human receptor, generally demonstrating full agonism with an A_{50} range of 0.1–30 nM (Sauty *et al*., 1999; Proost *et al*., 2001; Gonsiorek *et al*., 2003; Heise *et al*., 2005). CXCL9 and CXCL10 have been shown to behave as full or partial agonists depending upon the assay system tested with A_{50} ranges of 10–100 and 30–300 nM, respectively (Clark-Lewis *et al*., 2003; Gonsiorek *et al*., 2003; Heise *et al*., 2005). What is intriguing about CXCR3, in contrast to many other chemokine receptors, is that approximately 40% of freshly isolated human peripheral blood T cells express the receptor but these cells do not possess functional responsiveness to CXCR3 agonists (Loetscher *et al*., 1998). It has been demonstrated that activation of peripheral blood T cells *in vitro* induces responsiveness to CXCR3 agonists, through increasing receptor density (Loetscher *et al*., 1998). In addition, Xie *et al*. (2003) showed that murine T cells activated under Th2-polarizing conditions expressed high surface levels of CXCR3 and were able to migrate *in vitro* to CXCR3 agonists. However, following adoptive transfer to naive mice, these Th2 cells were not able to migrate to sites of inflammation, in contrast to Th1-polarized cells (Xie *et al*., 2003). These authors claim that antigen encounter but not cytokine milieu plays a dominant role in the regulation of CXCR3 expression levels. These data suggest that surface expression of CXCR3 does not necessarily predict *in vitro* and/or *in vivo* functional responsiveness of cells.

This study sets out to describe and validate an agonist-induced CXCR3 receptor internalization assay. Such assays have previously been used in a qualitative manner to elucidate the processes involved in chemokine receptor-trafficking events. Generally, total surface expression of chemokine receptors, in common with other members of the G-protein coupled receptor superfamily, is the net outcome of processes governing both loss (endocytosis and downregulation) and gain (re-expression and new synthesis) of receptor expression (Koenig and Edwardson, 1997). These processes may occur constitutively but, in the presence of agonist, the dynamic equilibrium of these events changes and receptors are rapidly endocytosed. CXCL11-induced CXCR3 receptor internalization has been reported to occur within a 30 min incubation period (Sauty *et al*., 2001). Furthermore, each CXCR3 agonist appears to utilize different intra- and extracellular domains for specific signalling and functional responses. Colvin *et al*. (2004) demonstrated that the carboxyl terminus of human CXCR3 was required for CXCL9- and CXCL10-induced CXCR3 internalization by mutagenesis studies, while the third intracellular loop of CXCR3 was required for CXCL11-induced CXCR3 internalization. Previous data from the same group demonstrated that CXCR3 internalization events were not affected by pretreatment with *Pertussis* toxin and were therefore independent of G-protein coupling (Sauty *et al*., 2001). Insensitivity to *Pertussis* toxin for receptor internalization events has been reported for other $G_{\alpha i}$-coupled chemokine receptors such as CXCR4 (Forster *et al*., 1998). Studies examining the extracellular components of CXCR3 required for signalling events suggest a multistep model of CXCR3 activation, similar to that reported for CCR2 receptors (Monteclaro and Charo, 1997; Xanthou *et al*., 2003; Colvin *et al*., 2004). The first step of receptor activation by all CXCR3 agonists involves high-affinity agonist binding to sulphated tyrosine residues within the amino terminus and while the extracellular domains required for chemotaxis have been identified, the corresponding extracellular residues involved in agonist-induced CXCR3 receptor internalization have not been fully elucidated (Colvin *et al*., 2004).

NBI-74330, a small molecule CXCR3 antagonist, has been studied using human CXCR3 GTPγS, calcium flux and cellular migration assays. The data demonstrate that NBI-74330 inhibited these human CXCR3-dependent processes with an IC_{50} range of 7–18 nM (Heise *et al*., 2005). A second molecule, TAK-779, while specific for human CCR5 only, demonstrated dual antagonism of murine CCR5 and CXCR3 *in vitro* (Gao *et al*., 2003). TAK-779 was also shown to significantly inhibit T-cell trafficking in a murine collagen-induced arthritis model, which may, in part, be due to antagonism of the murine CXCR3 receptor (Gao *et al*., 2003).

The murine CXCR3 receptor has not been extensively studied and characterized, often due to limitations of reagents at the time of publication. However, the generation of CXCR3- or CXCL10-deficient mice has implicated CXCR3 in driving models of viral inflammation of the CNS, transplant rejection and pulmonary fibrosis (Hancock *et al*., 2000, 2001; Christensen *et al*., 2004; Jiang *et al*., 2004; Hsieh *et al*., 2006). For example, CXCR3-deficient mice survived intracerebral lymphocytic choriomeningitis virus infection with susceptibility restored following reconstitution with wild-type $CD8^+$ T cells (Christensen *et al*., 2004). More recently, CXCL10-deficient mice have identified the key requirement of this agonist for immune surveillance of the CNS following lymphocytic choriomeningitis virus infection in CXCL10-deficient mice have been identified (Christensen *et al*., 2006). In contrast, intracerebral infection of CXCR3- or CXCL10-deficient mice with dengue virus showed

significantly higher mortality rates than wild-type mice, suggesting a protective role for CXCR3 and CXCL10 in such viral infections (Hsieh *et al*., 2006). CXCR3-deficient mice have also demonstrated profound resistance to acute cardiac rejection, with graft survival permanently maintained in these mice following treatment with a subtherapeutic dose of cyclosporin A (Hancock *et al*., 2000). Furthermore, the use of CXCL10-deficient recipient mice showed that donor-derived CXCL10 was responsible for allograft rejection (Hancock *et al*., 2001). Many of the gene-deletion studies expand upon data generated with anti-ligand antibodies, for example Hildebrandt *et al*. (2004) demonstrated that neutralization of CXCL9 or CXCL10 in a model of experimental idiopathic pneumonia syndrome, significantly inhibited donor cell recruitment to the lungs comparable to that demonstrated using CXCR3-deficient mice. Few studies have completely blocked the CXCR3 receptor in wild-type mice, although neutralization of murine CXCR3 using a polyclonal antibody was carried out in a sheep red blood cell delayed-type hypersensitivity model. While 70% inhibition was observed in the anti-CXCR3 antibody treatment group it was not fully determined whether the antibody had cell-depletion properties that may have contributed to the apparent efficacy (Xie *et al*., 2003).

There are caveats to many of the approaches undertaken to validate CXCR3 in inflammatory disease conditions. Elucidation of the feasibility of pharmacological manipulation of CXCR3 in chronic inflammatory diseases awaits therapeutic blockade of the receptor using small molecule antagonists. Here, we describe the characterization of an agonist-induced CXCR3 receptor internalization assay in activated primary murine cells, which has been used to determine agonist potency and antagonist affinity measurements and most importantly for PK/PD analyses enabling discrimination between dosing regimens for preclinical validation of CXCR3 as a drug target.

Methods

Animal use

Adult mice (6–8 weeks of age) were used in accordance with the Animals (Scientific Procedures) Act 1986. Balb/c mice were purchased from Charles River Laboratories (Margate, UK) and DO11.10 mice were obtained from the John Radcliffe Hospital (Oxford, UK). Animals were kept under a light/dark cycle of 12/12 h and had access to food and water *ad libitum*.

Mouse blood was collected into Microvette 600 EDTA tubes (Sarstedt, Leicester, UK) via cardiac puncture under terminal gaseous anaesthesia (isoflurane; NVS, Stoke-on-Trent, UK). For PK/PD experiments, male Balb/c mice were dosed with 100 μl of dosing solution either via oral gavage (25 mm; 20 G cannula) (Harvard Apparatus, Edenbridge, UK) or s.c. using a 25 G needle (BD Biosciences, Oxford, UK). In each case, the vehicle used for dosing was 0.1% sodium docusate/99.9% methylcellulose (0.5%; 400 cP). EDTA-treated naive, Balb/c, sex-matched, plasma was purchased from B&K (Hull, UK).

Cell culture

Spleens from DO11.10 mice were collected and single-cell splenocyte suspensions were generated following disaggregation through a 40-μm mesh (BD Biosciences). Cells were washed twice in DO11.10 medium (RPMI + 10% fetal bovine serum + penicillin (100 U ml^{-1})–streptomycin (0.1 mg l^{-1}) + L-glutamine (2 mM) + 50 μM 2-mercaptoethanol + 12.5 mM HEPES) (Sigma-Aldrich, Dorset, UK), counted and resuspended at 1×10^6 cells ml^{-1} in DO11.10 medium containing antigen (ovalbumin$_{323-339}$, 200 ng ml^{-1}) (University of Southampton, Southampton, UK). Three days later, cells were split twofold and resuspended in fresh DO11.10 medium reconstituted with recombinant murine interleukin-2 (rmuIL-2, 10 ng ml^{-1}) (Peprotech, London, UK). Cells were cultured for a further 5 days prior to use in the receptor internalization assay.

Murine CXCR3 internalization assay

Activated DO11.10 cells, as described above, were pelleted and washed in fresh DO11.10 medium. Cells were pooled, resuspended in medium, overlaid onto sterile Nycoprep (1.077 Å) (Axis Shield, Huntingdon, UK) and centrifuged at 550 *g* for 20 min at room temperature. Viability of cells present at the interface was determined by Trypan blue exclusion. Cells were removed from the interface and washed twice in assay buffer (0.25% BSA in phosphate-buffered saline). Cells (5×10^5) were incubated in a total assay volume of 100 μl, which included the agonist and antagonist concentrations as required, at 37° C for the specified time. A 60 min incubation period was used in all cases, with the exception of time-course studies. For detection of surface CXCR3 expression levels, cells were washed and stained with rhodamine–phycoerythrin-conjugated anti-murine CXCR3 or isotype control antibodies at a concentration of 2.5 μg ml^{-1} for 30 min on ice (R&D Systems, Abingdon, UK; Invitrogen, Paisley, UK). Unbound antibody was then removed by washing and the cells were fixed using CellFix according to manufacturer's instructions (BD Biosciences), prior to data acquisition using an EPICS-XL flow cytometer (Beckman Coulter, High Wycombe, UK). Specific CXCR3 staining was determined by subtracting the isotype control staining profile for each experimental condition.

For plasma assays, 5×10^5 cells were pelleted and resuspended in 90 μl of sex-matched EDTA-treated mouse plasma. For *in vitro* plasma assays, the plasma source was naive pooled Balb/c plasma. For *ex vivo* PD studies, plasma was obtained from mouse blood at appropriate time intervals following *in vivo* dosing of CXCR3 antagonist and at each time point the plasma was pooled. Assays were then carried out in a total volume of 100 μl, at 37° C for 60 min. Surface CXCR3 was detected as described previously.

[^{35}S]GTPγS-binding assay

Membranes from murine CXCR3-transfected Chinese Hamster ovary cells were prepared as follows: cell pellets were resuspended at 1×10^7cells ml^{-1} and homogenized using a glass 10 ml manual homogenizer in ice-cold buffer A (15 mM Tris-HCl, 2 mM MgCl, 0.3 mM EDTA, 1 mM EGTA, pH 7.5). The homogenate was centrifuged at 40 000 *g* for 25 min at

4° C. The supernatant was carefully removed and the pellet resuspended in buffer A and centrifuged as outlined previously. The supernatant was then removed and the final pellet resuspended at 1×10^8 cells ml^{-1} in ice-cold buffer B (7.5 mM Tris-HCl, 12.5 mM MgCl, 0.3 mM EDTA, 1 mM EGTA, 250 mM sucrose, pH 7.5). The protein concentration was determined using BCA Protein Assay Kit according to manufacturer's instructions (Perbio Science, Cramlington, UK). The membrane preparation was divided into aliquots, frozen and stored at −80° C until use.

The GTPγS-binding assay was carried out in a 96-well Optiplate (Perkin Elmer, Beaconsfield, UK) in a final assay volume of 200 μl, using 1 μg per well of cell membrane resuspended in binding buffer (20 mM HEPES, 100 mM NaCl, 10 mM MgCl, 1 mM EDTA (pH 7.4), 5 μM GDP, 25 $\mu g\,ml^{-1}$ saponin, 5 $mg\,ml^{-1}$ wheat germ agglutinin–polyvinyl toluene scintillation proximity assay beads, 0.1% BSA) and preincubated with agonist (in the absence and presence of antagonist or antibody) at room temperature for 60 min. At this time, 0.3 nM [^{35}S]GTPγS (Amersham, Little Chalfont, UK) was added and incubated for a further 2 h at room temperature before centrifugation for 10 min at 380 *g*. Bound radioactivity was measured using a TopCount NXT microplate scintillation and luminescence counter (Perkin Elmer).

Bioanalysis of NBI-74330 and metabolite-1

Blood and plasma levels of NBI-74330 and metabolite-1 were measured using HPLC-MS/MS. Samples (20 μl) were dispensed into a 96-deep well plate (Porvair, King's Lynn, UK) and measured against calibration standards. Samples and calibration standards were precipitated with internal standard in acetonitrile (120 μl), mixed and then centrifuged at 1750 *g* at 4° C for 10 min. Blood and plasma sample extracts were then analysed using a Micromass Mass Spectrometer (Waters Ltd, Elstree, UK). Extracts (20 μl) were injected using a CTC analytics HTS Pal Autosampler (Presearch, Hitchin, UK) onto a Phenomenex Luna C18 50 mm × 2.1 mm, 5 μm column (Phenomenex, Macclesfield, UK) operated at 40° C and at an eluent flow rate of 1.0 $ml\,min^{-1}$ with a split ratio of 5:1 into the mass spectrometer. Analytes were eluted using a high-pressure linear gradient programme by means of an HP1100 binary HPLC system (Agilent Technologies, Stockport, UK) using water containing 0.1% formic acid (solvent A) and acetonitrile containing 0.1% formic acid (solvent B).

A 5 min gradient was used for analysis of *in vivo* blood and plasma extracts, increasing from 5 to 95% solvent B at 4 min before returning to the starting conditions at 4.1 min, which were maintained until 5 min.

A 3 min gradient was used for analysis of plasma protein-binding extracts, which increased from 5 to 95% solvent B at 2 min before returning to the starting conditions at 2.1 min, which were maintained until 3 min.

Plasma protein-binding properties of NBI-74330

Plasma protein binding of NBI-74330 was measured by equilibrium dialysis using a 96-well Teflon block (HT Dialysis LLC, Gales Ferry, CT, USA). Membranes (3-kDa cutoff) were conditioned in deionized water for 60 min, followed by 80:20 deionized water/ethanol for 20 min, and then rinsed in deionized water before use. Plasma was mixed with test compound (10 μM) and 50 μl aliquots ($n = 6$ replicate determinations) were loaded onto the 96-well equilibrium dialysis block. Dialysis vs phosphate buffer (100 mM, pH 7.4, 50 μl) was carried out for 4 h at 37° C with constant agitation, after which time, aliquots of plasma and buffer were transferred to a 96-deep well plate. The composition in each well was balanced with control fluid, such that the volume of buffer and plasma was the same in each sample. Sample extraction was performed by the addition of 120 μl of acetonitrile containing internal standard. Samples were mixed, centrifuged at 1750 *g* at 4° C for 10 min and 40 μl of supernatant was transferred into another 96-well plate followed by addition of 160 μl of 5% acetonitrile (in water). Analysis of test compound was performed using HPLC-MS/MS as described and relative responses of test compound in the buffer and plasma half-wells were used to determine the respective drug-free fraction.

Data analysis and statistics

Agonist concentration effect (E/[A]) curves were fitted to a three-parameter logistic equation, using GraphPad Prism (version 4). Data (mean ± s.e.) from individual experiments are shown superimposed with a single curve generated using the mean of the individual parameter estimates ($n \geqslant 3$). The control E/[A] curve parameters, midpoint location ($[A]_{50}$), midpoint slope (n_H) and maximal asymptote (α), were not significantly different between individual experiments and the mean values for each control group depicted, lie within 95% confidence limits of the population (CXCL11 buffer $pA_{50} = 9.38 \pm 0.31$, $n = 32$; plasma $pA_{50} = 9.07 \pm 0.21$, $n = 35$; data expressed as mean ± s.d.) calculated from a number of experiments conducted over a 14-month time period by independent operators.

Specific experiments were conducted for Schild analysis and E/[A] curves were constructed in the presence and absence of increasing antagonist concentrations. A competitive antagonist will shift E/[A] curves to the right with no significant change in E/[A] curve midpoint slope or maximum response, as judged by using one-way ANOVA with Bonferroni post-test. If no significant changes were obtained, individual dose ratios (DRs) were calculated from the degree of rightward shift of the control E/[A] curve in the presence of antagonist and fitted to the following equation:

$$\log(DR - 1) = \text{Schild slope} \cdot \log[\text{antagonist}] - pK_B$$

If the unconstrained Schild slope (b) was not significantly different from unity, the data were re-fitted constraining the slope to unity and pK_B was determined. If the criteria of competitive antagonism were not fully satisfied, an apparent pA_2 value was estimated from the lowest antagonist concentration that produced a significant rightward shift of the E/[A] curve.

Drugs

NBI-74330 was synthesized as described elsewhere (Medina and Johnson, 2002). Metabolite-1 was prepared by reaction of NBI-74330 (1.20 g) with metachloroperbenzoic acid (0.48 g) (Schneller and Luo, 1980) and the product was

purified by preparative HPLC to give the compound as a colourless solid (0.85 g).

Results

In vitro *characterization of an agonist-induced murine CXCR3 internalization assay*

Murine DO11.10 splenocytes activated *in vitro* for 8 days displayed higher levels of surface CXCR3 expression (66 ± 2%, $n=6$; Figure 1a) compared to freshly isolated splenocytes (30 ± 1%, $n=4$; data not shown). Surface CXCR3 expression was significantly (ANOVA; $P<0.01$ ($n=6$)) reduced following 60 min incubation at 37° C with a single concentration (300 nM) of each of the CXCR3 agonists (CXCL9, CXCL10 and CXCL11), but was not significantly affected by incubation with 300 nM CXCL12, a CXCR4 receptor agonist (Figure 1b). The time course and concentration dependence of agonist-induced loss of surface CXCR3 expression showed that for each CXCR3 agonist, a 60 min

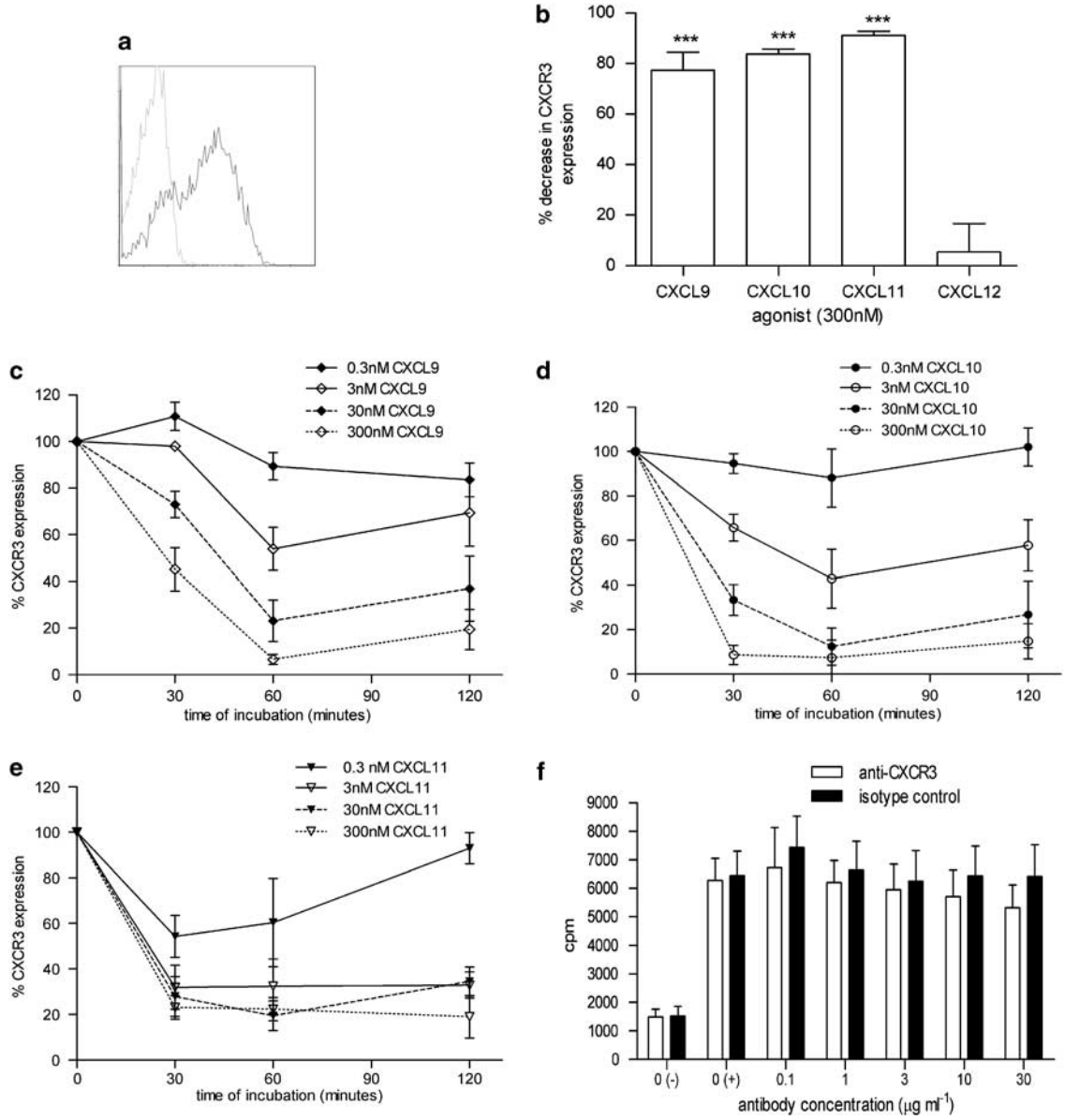

Figure 1 The selectivity and specificity of a murine CXCR3 internalization assay. (**a**) CXCR3 surface expression on DO11.10 cells activated *in vitro* with antigen (ovalbumin$_{323-339}$) was measured by flow cytometry using anti-CXCR3 antibody (black line) compared to isotype control staining (dashed line). (**b**) A single concentration (300 nM) of CXCL9, CXCL10, CXCL11 and CXCL12 was incubated with activated DO11.10 cells for 60 min at 37° C and the percentage decrease in surface CXCR3 expression was measured compared to cells incubated with buffer alone (***$P<0.001$; $n=3$–14). (**c–e**) CXCL9, CXCL10 and CXCL11 concentrations (0.3, 3, 30 and 300 nM) were incubated with activated DO11.10 cells for 30, 60 or 120 min and CXCR3 expression was compared to cells incubated with buffer alone (100% CXCR3 expression) at each time point ($n=3$). (**f**) Membranes generated from muCXCR3-transfected Chinese Hamster ovary cells were incubated with 0.1 nM CXCL11 ± anti-CXCR3 antibody or isotype control antibody (rat IgG2a) for 60 min and then incubated with 0.3 nM [^{35}S]GTPγS for 2 h followed by measurement of GTP binding ($n=3$). The negative control, 0(−), was carried out in the absence of agonist while all other samples were incubated with 0.1 nM CXCL11.

incubation time was sufficient to achieve steady-state responses (Figures 1c–e).

The specificity of the agonist-induced loss of surface CXCR3 expression was explored by determining whether the loss of measured surface CXCR3 expression was due to a competitive interaction between the anti-CXCR3 antibody and CXCL11. This was investigated, using a murine CXCR3 GTPγS assay to determine the effect of a range of anti-CXCR3 antibody concentrations (1–30 μg ml^{-1}) or isotype control antibody on CXCL11 binding to cell membranes expressing murine CXCR3 (Figure 1f). Individual antibody concentrations were investigated in the presence and absence of a single CXCL11 concentration, 0.1 nM, equivalent to an A_{50} in this assay (data not shown). No significant inhibition of CXCL11 binding by the anti-CXCR3 antibody was observed compared to the isotype control antibody. This indicated that the antibody concentration (2.5 μg ml^{-1}) used to detect surface CXCR3 expression in the receptor internalization assay was not competing with CXCL11 for the same binding site.

Classification of murine CXCR3 using the CXCL11-induced receptor internalization assay

E/[A] curves were constructed using a 60 min incubation period. CXCL11 exhibited the greatest potency (pA_{50} = 9.23 ± 0.26, n = 12), while CXCL10 (pA_{50} = 7.74 ± 0.13, n = 14) and CXCL9 (pA_{50} = 7.51 ± 0.38, n = 6) were 30- to 50-fold less potent. The maximal responses in the E/[A] curve for each agonist were equivalent (Figure 2a).

In a separate set of experiments, a small molecule CXCR3 receptor antagonist, NBI-74330 (Heise *et al*., 2005), was used to further characterize the CXCL11-induced loss of surface CXCR3 expression. CXCL11 E/[A] curves were generated in the presence and absence of increasing concentrations of NBI-74330 (Figure 2b). NBI-74330 (30–300 nM) produced concentration-dependent, parallel rightward shifts of the CXCL11 E/[A] curve with no significant change in the E/[A] curve maximal response (Figure 2b). However, at the highest concentration (1 μM), a significant reduction of the CXCL11 E/[A] curve maximal response was obtained (ANOVA; P<0.05), which was

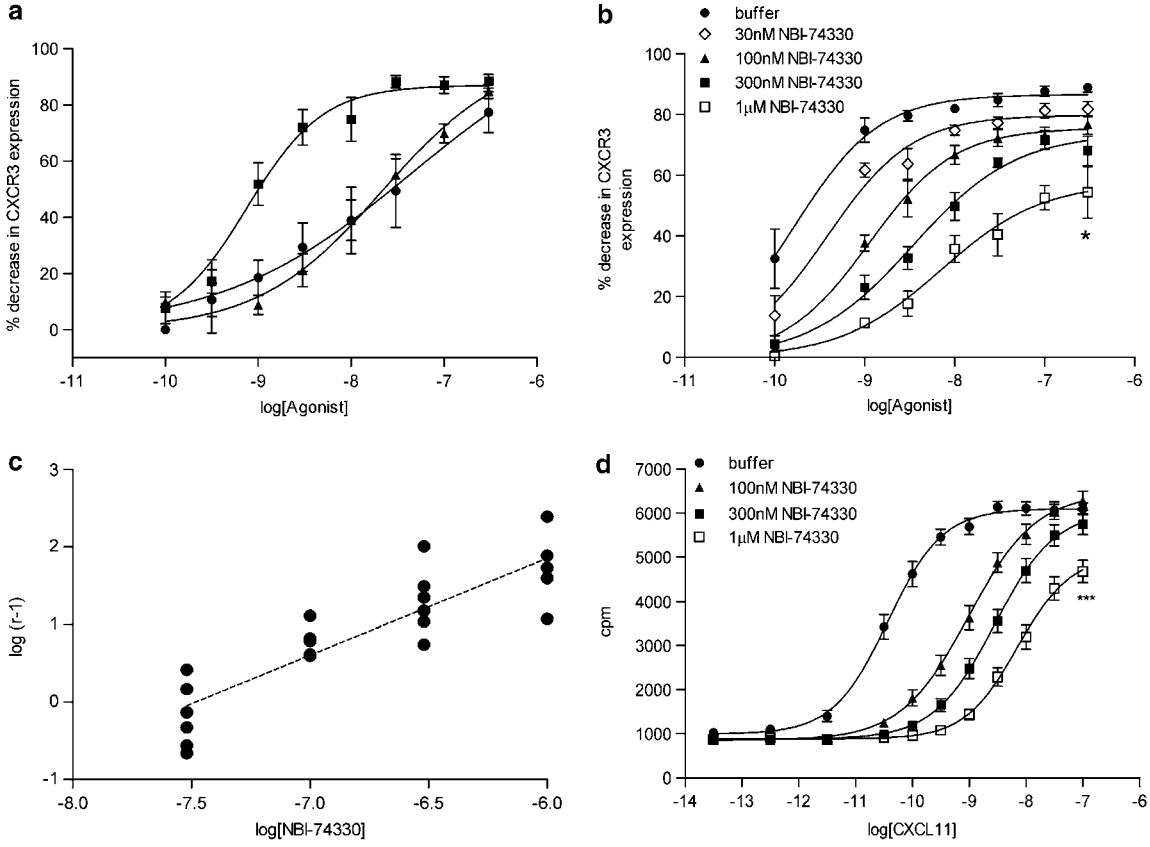

Figure 2 Murine CXCR3 receptor classification using receptor internalization and GTPγS assays. (**a**) Increasing agonist concentrations (0.1–300 nM) were incubated with activated DO11.10 cells for 60 min at 37° C and surface CXCR3 expression was detected by flow cytometry. Data are expressed as percent decrease in CXCR3 expression (mean ± s.e.) to generate E/[A] curves for CXCL11, CXCL10 and CXCL9 (n = 6–14). (**b**) Increasing concentrations of NBI-74330 (30 nM–1 μM) were included in the CXCR3 internalization assay and CXCL11 E/[A] curves were generated following 60 min incubation at 37° C. Data are expressed as percent decrease in CXCR3 expression (mean ± s.e.) in the presence and absence of 30, 100, 300 nM or 1 μM NBI-74330 (n = 6) (*P<0.05). (**c**) Schild plot analysis comparing the degree of rightward shift of the CXCL11 E/[A] curve (log (r−1)) in the presence of NBI-74330 concentrations to the CXCL11 E/[A] curve generated in the absence of antagonist. Individual data points are plotted, the unconstrained Schild slope is b = 1.25 ± 0.14. An apparent pA_2 value of 7.84 ± 0.14 was estimated from the 100 nM NBI-74330 E/[A] curve (n = 6). (**d**) Increasing concentrations of NBI-74330 (100 nM–1 μM) were included within the murine CXCR3 GTPγS assay using the agonist CXCL11. Data are expressed as mean c.p.m. ± s.e. in the presence and absence of 100, 300 nM or 1 μM NBI-74330 (n = 3) (***P<0.001). An apparent pA_2 value of 8.35 ± 0.04 was estimated from the 100 nM NBI-74330 E/[A] curve.

accompanied by a significant flattening of the E/[A] curve midpoint slope (ANOVA; $P<0.001$). Although the unconstrained Schild slope was not significantly different from unity ($b=1.25\pm0.14$, $n=6$) (Figure 2c), the criteria for competitive antagonism were not fully satisfied (Jenkinson, 1991). Consequently, an apparent pA_2 value of 7.84 ± 0.14 ($n=6$) was determined from the lowest antagonist concentration (100 nM) that produced a significant rightward shift of the CXCL11 E/[A] curve.

For comparison, the NBI-74330–CXCL11 interaction was studied using a murine GTPγS assay. CXCL11 E/[A] curves were obtained in the presence and absence of increasing concentrations of NBI-74330 (100 nM–1 μM). NBI-74330 produced concentration-dependent, parallel rightward shift of the CXCL11 E/[A] curve (Figure 2d). However, at the highest concentration of 1 μM NBI-74330, a significant reduction of the CXCL11 E/[A] curve maximal response was observed (ANOVA; $P<0.001$) (Figure 2d). Again, although the unconstrained Schild slope was not significantly different from unity ($b=0.89\pm0.05$, $n=3$), the behaviour was not consistent with the expectations for competitive antagonism. Therefore, an apparent pA_2 value of 8.35 ± 0.04 ($n=3$) was obtained.

Compatibility of the murine CXCR3 internalization assay with plasma

To determine the utility of the murine CXCR3 internalization assay for PK/PD modelling, we investigated the inclusion of whole blood or plasma within the assay system. The magnitude of basal CXCR3 expression was substantially reduced in mouse whole blood (data not shown), whereas the basal receptor expression was unchanged by the presence of mouse plasma. The impact of mouse plasma on agonist potency and antagonist affinity estimates was determined; CXCL11 demonstrated similar potency in the presence and absence of mouse plasma (pA_{50} values: buffer 9.23 ± 0.26, $n=12$; plasma 9.17 ± 0.15, $n=16$; Figure 3a), with no significant change in the E/[A] curve midpoint slope or maximal response. Consequently, CXCL11 was employed for all subsequent experiments. In a separate set of experiments, plasma CXCL11 E/[A] curves were generated in the presence and absence of increasing concentrations of NBI-74330. NBI-74330 (1–10 μM) produced concentration-dependent, parallel rightward shift of the CXCL11 E/[A] curve, with no significant change in the E/[A] curve maximal response (Figure 3b). The relationship between the degree of rightward shift of the CXCL11 E/[A] curve and the concentration

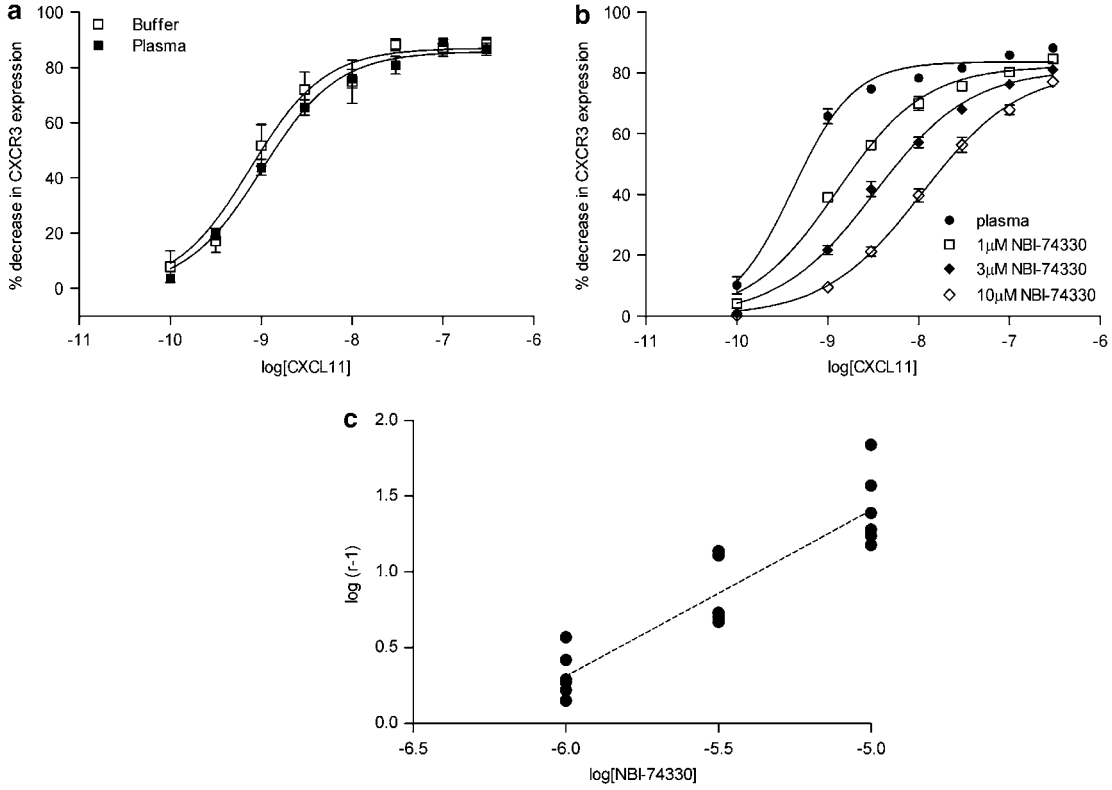

Figure 3 Tolerance of the murine CXCR3 internalization assay to plasma. (**a**) CXCL11 E/[A] curves were generated following 60 min incubation at 37° C of agonist with activated DO11.10 cells in the presence ($n=16$) and absence ($n=12$) of 90% EDTA-treated, naive mouse plasma, followed by surface CXCR3 staining by flow cytometry. (**b**) Increasing concentrations of NBI-74330 (1–10 μM) were included within the CXCR3 internalization assay and CXCL11 E/[A] curves were generated following 60 min incubation at 37° C. Data are expressed as percent decrease in CXCR3 expression (mean ± s.e.) in the presence and absence of 1, 3 or 10 μM NBI-74330 ($n=6$). (**c**) Schild plot analysis comparing the degree of rightward shift of the CXCL11 E/[A] curve in the plasma receptor internalization assay format, in the presence of NBI-74330 concentrations to the CXCL11 E/[A] curve generated in the absence of antagonist ($n=6$). Individual data points are plotted and the unconstrained Schild slope was $b=1.10\pm0.12$. Constraining the Schild slope to a value of unity generated a pK_B value of 6.36 ± 0.01.

of NBI-74330 was linear and an unconstrained Schild slope ($b = 1.10 \pm 0.12$, $n = 6$) not significantly different from unity was obtained (Figure 3c). Constraining the Schild slope to a value of unity, generated a pK_B value of 6.36 ± 0.01 ($n = 6$), demonstrating a ~30-fold reduced affinity of NBI-74330 for murine CXCR3 receptor in the presence of plasma compared to that using buffer in the receptor internalization assay.

PK and PD profiles of the CXCR3 antagonist, NBI-74330 following administration to mice

The murine PK profile of NBI-74330 (100 mg kg^{-1}) was determined following p.o. and s.c. administration and analysis of blood samples by HPLC-MS/MS (Figures 4a and 5a, respectively). NBI-74330 blood exposure was greater following p.o. compared to s.c. administration, as indicated by maximum concentration (C_{max}) (p.o. 7051–13,010 ng ml^{-1}; s.c. 1047–4737 ng ml^{-1}; data shown as ranges) and area under the curve (p.o. 21,603–41,349 ng h ml^{-1}; s.c. 5702–21,600 ng h ml^{-1}; data shown as ranges). However, dosing of NBI-74330 (Figure 4b) generated an N-oxide metabolite (metabolite-1; Figure 4c) that was active against murine CXCR3, and apparent pA_2 values for metabolite-1 were calculated from the effects of a single antagonist concentration in the CXCR3 receptor

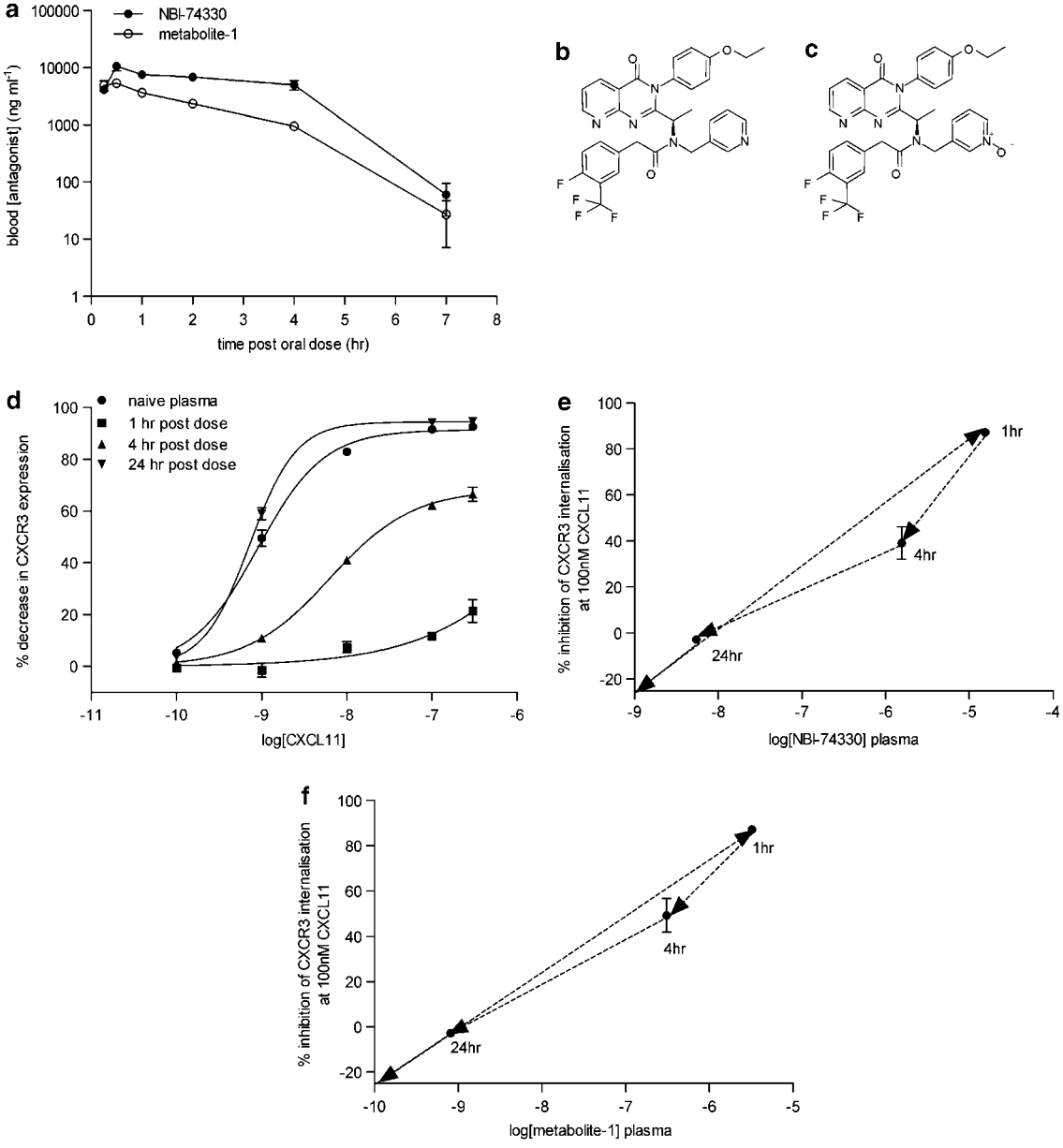

Figure 4 PK/PD parameters of NBI-74330 (100 mg kg^{-1}) following oral administration to mice. (**a**) Blood concentration of NBI-74330 and metabolite-1 at time (h) post-oral dose of 100 mg kg^{-1} of NBI-74330 in 0.1% sodium docusate/99.9% methyl cellulose ($n = 3$). (**b** and **c**) Chemical structures of NBI-74330 and metabolite-1. (**d**) Effect of plasma samples taken at 1, 4 and 24 h post-oral dose with 100 mg kg^{-1} NBI-74330 on CXCL11-induced CXCR3 internalization response compared to the E/[A] curve generated in naive mouse plasma ($n = 3$). (**e** and **f**) PK/PD relationship of NBI-74330 and metabolite-1, respectively, following oral administration of NBI-74330 (100 mg kg^{-1}). Data are presented as plasma concentration of each antagonist at 1, 4 and 24 h post p.o. dose compared to the degree of inhibition of the CXCR3 internalization response induced by 100 nM CXCL11 ($n = 3$).

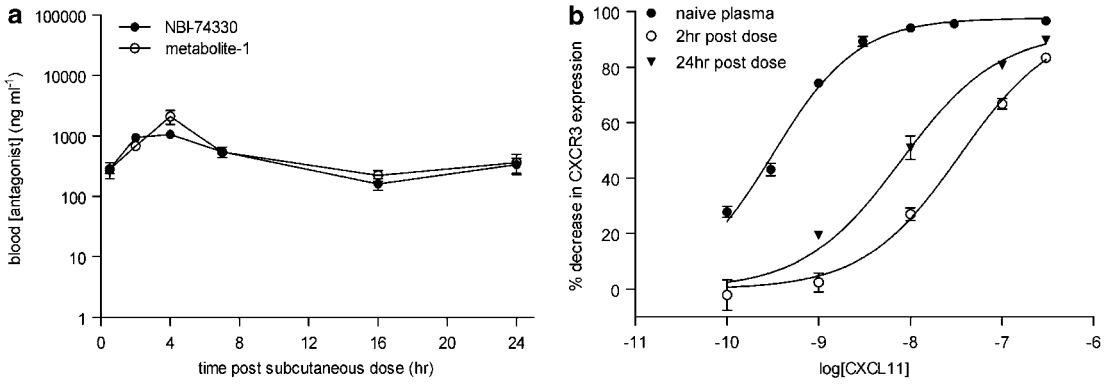

Figure 5 PK/PD parameters of NBI-74330 (100 mg kg^{-1}) following subcutaneous administration to mice. (**a**) Blood concentration of NBI-74330 and metabolite-1 at time (h) post-subcutaneous dose of 100 mg kg^{-1} of NBI-74330 in 0.1% sodium docusate/99.9% methyl cellulose ($n=3$). (**b**) Effect of plasma samples taken at 2 and 24 h post-subcutaneous dose with 100 mg kg^{-1} NBI-74330 on CXCL11-induced CXCR3 internalization response compared to the E/[A] curve generated in naive mouse plasma ($n=3$).

internalization assay (buffer pA_2: 7.42 ± 0.10 ($n=3$); plasma pA_2: 7.04 ± 0.16 ($n=3$); data not shown). Blood C_{max} for metabolite-1 was higher following p.o. compared to s.c. administration (p.o. 4846–6276 ng ml^{-1}; s.c. 1005–2842 ng ml^{-1}) while the area under the curve was similar between dosing regimens (p.o. 8149–14,495 ng h ml^{-1}; s.c. 8897–17,704 ng h ml^{-1}) as a consequence of the prolonged profile of both NBI-74330 and metabolite-1 following s.c. administration, with significant concentrations of both antagonists maintained at 24 h post-dose (Figure 5a).

The corresponding PD readout, the degree of antagonism of the CXCL11 E/[A] curve, was measured using plasma collected at fixed time points (1, 4 and 24 h) following p.o. administration of NBI-74330 (100 mg kg^{-1}). Significant antagonism of the CXCL11 E/[A] curve (>30-fold rightward shift; ANOVA; $P<0.01$ ($n=3$)) was obtained at 1 and 4 h but not at 24 h post-administration of NBI-74330 p.o. (Figure 4d). PK/PD analysis for NBI-74330 and metabolite-1 following p.o. administration did not demonstrate hysteresis but showed a linear relationship, indicating a direct relationship between exposure and effect (Figures 4e and f, respectively). In addition, following s.c. administration of NBI-74330, the corresponding PD readout was determined at 2 and 24 h post-dose and significant antagonism of the CXCL11 E/[A] curve (>30-fold rightward shift; ANOVA; $P<0.001$) was obtained at both time points (Figure 5b). This PK/PD analysis suggested that, compared to p.o. dosing, s.c. administration of NBI-74330 would generate a more prolonged CXCR3 receptor antagonism *in vivo*.

Discussion

Understanding the role and effect of antagonism of CXCR3 in preclinical models of chronic inflammation helps to determine the pharmacological feasibility of this target in a drug discovery environment. We therefore set out to develop a cell assay that would discriminate between small molecule CXCR3 antagonists within a research-screening cascade. To our knowledge, this study provides the first example of applying receptor pharmacology principles to a chemokine receptor internalization assay and using this to generate PK/PD information to discriminate between dosing regimens.

For many G-protein coupled receptors, receptor internalization assays have been described to help assign newly identified agonists to their appropriate receptor(s) and to determine agonist potency orders. The selectivity of the murine CXCR3 internalization response was demonstrated using the CXCR3 agonists, CXCL9, CXCL10 and CXCL11, compared to the CXCR4 agonist CXCL12, and showed that only the CXCR3 agonists modulated surface expression of CXCR3 (Figure 1b). The extracellular domains of murine CXCR3 recognized by the CXCR3 antibody or CXCL11, used in our assay, have not been fully characterized. However, further examination of the specificity of the receptor internalization assay showed that altered surface CXCR3 detection was not due to hindrance of antibody staining by CXCL11 binding to the receptor (Figure 1f). In agreement with similar receptor internalization studies, our findings demonstrate that CXCR3 agonists decrease the proportion of surface-expressed CXCR3 on activated murine cells in a concentration- and time-dependent manner (Dorland *et al.*, 1979; Arai *et al.*, 1997; Sauty *et al.*, 2001). Interestingly, CXCL10 and CXCL11 reached the maximal internalization response within 30 min of incubation, while CXCL9 reached maximal effect by 60 min (Figures 1c–e). Sauty *et al.* (2001) previously reported that human CXCL11 induced rapid internalization of human CXCR3 with maximal effects within a similar time frame to that observed for murine CXCR3. CXCL9 has been described as a partial agonist in a human CXCR3 receptor internalization assay (Sauty *et al.*, 2001), although a prolonged incubation time may have been required by CXCL9 in this instance. The delayed response of CXCL9-induced internalization of murine CXCR3, compared to CXCL10 and CXCL11, may be due to utilization of different receptor domains. Distinct receptor domains have been described for CXCL9-, CXCL10- and CXCL11-induced human CXCR3 internalization events (Colvin *et al.*, 2004), while those required for murine CXCR3 internalization responses have not been identified. The murine CXCR3 internalization assay also showed that CXCL11 was at least 30-fold more potent than either CXCL10 or CXCL9

(Figure 2a), which is in agreement with studies examining the human CXCR3 agonist potency order (Clark-Lewis *et al*., 2003; Heise *et al*., 2005). The potency of CXCL11 and its tolerance of plasma in the assay allowed a large experimental window for antagonism of the CXCR3 receptor internalization response using both *in vitro* and *ex vivo* assay formats. The effect of different anticoagulants in mouse plasma did not significantly affect CXCL11-induced CXCR3 receptor internalization, while the potency of CXCL10 was decreased in EDTA-treated plasma and completely inhibited by heparinized plasma (data not shown), presumably due to the heparin-binding domains possessed by CXCL10 (Campanella *et al*., 2003). Therefore, the use of CXCL11 for further studies provided technical flexibility within the assay.

Further classification of murine CXCR3 with the receptor internalization assay employed Schild analysis using a known human CXCR3 small molecule antagonist NBI-74330 (Heise *et al*., 2005). This antagonist had previously been studied in GTPγS, calcium flux and chemotaxis assays using cell lines expressing human CXCR3 and generated IC_{50} values against human CXCL11 of 5.5, 7 and 3.9 nM, respectively. In addition, Heise *et al*. (2005) reported that NBI-74330 demonstrated insurmountable antagonism in both human CXCR3 calcium flux and GTPγS assays. In both assays, the profile of NBI-74330 antagonism showed a concentration-dependent reduction of the maximal response without rightward shift of the CXCL11 E/[A] curve (Heise *et al*., 2005). However, at the murine CXCR3 receptor, we observed a different antagonism profile of the CXCL11 response by NBI-74330 in GTPγS and receptor internalization assays (Figures 2b and d). Significant rightward shift (1.88 log units) of the GTPγS E/[A] curve was obtained with 300 nM NBI-74330 without concomitant reduction in the E/[A] curve maximal response, whereas 1 μM NBI-74330 further rightward shifted the E/[A] curve (2.28 log units) and significantly reduced the maximal response. This profile was also obtained in the murine CXCR3 receptor internalization assay. Significant rightward shift (1.33 log units) of the CXCR3 receptor internalization E/[A] curve was obtained with 300 nM NBI-74330 without concomitant reduction of the E/[A] curve maximal response, whereas 1 μM NBI-74330 further rightward shifted the E/[A] curve (1.64 log units) and significantly reduced the maximal response. In both murine CXCR3 assays, the E/[A] curves generated in the presence of 1 μM NBI-74330 had a pA_{50} value of 8.15, suggesting that this may be related to the degree of receptor reserve within the assays (Figures 2b and d, respectively). Insurmountable antagonism, which is a concentration-dependent reduction of the E/[A] curve maximal response, with or without rightward shift of the CXCL11 E/[A] curve, has been described extensively within the literature for a wide range of receptor systems such as angiotensin II receptors (Pendleton *et al*., 1989), α_1-adrenoceptors (Blue *et al*., 1995) and 5-HT_2 receptors (Kaumann and Frenken, 1985). Historically, insurmountable antagonism was recognized to be due to a variety of mechanisms, both receptor and non-receptor mediated (Schild, 1949; Gaddum *et al*., 1955). A number of different explanations exist within the literature; irreversible competitive antagonism (Furchgott R, 1966), pseudo-irreversible antagonism (Paton and Rang, 1965), allosteric modulation (Kaumann and Frenken, 1988), a heterogenous receptor population or antagonist-induced reduction in the function of existing receptors (Liu *et al*., 1992; Robertson *et al*., 1994), which account for saturable and non-saturable insurmountable antagonism. Further pharmacological analyses, such as receptor protection and 'washout' studies, could be employed to determine whether the reduction in the CXCL11 E/[A] curve by NBI-74330 in common with the rightward shift of the CXCL11 E/[A] curve is due to a reversible, syntopic mechanism. Nevertheless, the affinity estimates for NBI-74330 calculated as apparent pA_2 values in our murine CXCR3 receptor internalization and GTPγS assays were 7.84 ± 0.14 and 8.35 ± 0.04, respectively, which are consistent with the values obtained at human CXCR3 receptors (Heise *et al*., 2005). In addition, the antagonism of CXCL11-mediated migration of activated DO11.10 cells was also investigated (data not shown). Interestingly, CXCL11 was ~30-fold less potent compared to receptor internalization assay, suggesting that the cell migration response is poorly coupled. Consequently, this limited the experimental window available in which the criteria for competitive antagonism was to be fully tested. Not withstanding this, an apparent pA_2 value (7.42 ± 0.05, $n = 3$) was obtained (data not shown), which was similar to the values obtained in the receptor internalization and GTPγS assays.

The murine CXCR3 receptor internalization assay tolerated plasma and permitted the generation of affinity estimates using CXCL11 as the agonist (Figure 3a). Subsequent Schild analysis of NBI-74330 generated an affinity estimate (pK_B value 6.36 ± 0.01), which was ~30-fold lower than in the absence of plasma. In addition, the antagonist concentration range employed did not demonstrate a reduction in the CXCL11 E/[A] curve maximal response (Figure 3b). This is consistent with expectations based on the degree of rightward shift of the CXCL11 E/[A] curves in this study compared to the corresponding study in buffer. The maximal degree of rightward shift obtained in the plasma assay format (1.42 log units) was within the range (<1.64 log units) outlined previously in the buffer receptor internalization assay where there was no concomitant reduction of the E/[A] curve maximal response. Interestingly mouse plasma protein binding for NBI-74330 was estimated at 97.3% (±0.5%) suggesting that in the presence of plasma only 2–3% of any NBI-74330 concentration is available for receptor binding. This may explain the 30-fold difference in affinity estimated for NBI-74330 in the absence and presence of plasma.

Dosing of NBI-74330 to mice yielded the formation of a previously unreported active metabolite (metabolite-1). The exposure profiles of parent (NBI-74330) and metabolite (metabolite-1) tracked with each other over time and a linear PK/PD relationship was demonstrated following p.o. dosing of NBI-74330 ($100\,mg\,kg^{-1}$) (Figures 4e and f). Hysteresis of the PK/PD relationship is often observed with the formation of an active metabolite leading to a delayed effect over time (Campbell, 1990). However, because the exposure profiles for each antagonist are parallel, one hypothesis for the linear PK/PD relationship is that there is rapid inter-conversion between NBI-74330 and metabolite-1 (Figures 4a and 5a). Comparison of dosing regimen by

adapting the CXCR3 internalization assay into an *ex vivo* format enabled distinction between p.o. and s.c. administration of NBI-74330. Oral dosing of NBI-74330 demonstrated slightly higher exposure levels of parent compared to metabolite-1 (threefold), while both antagonist profiles were equivalent following subcutaneous administration. This may reflect some saturation of metabolic activity resulting from the higher concentrations of NBI-74330 obtained following p.o. administration.

Previously, blockade of the CXCR3 receptor axis *in vivo* has relied on (1) deletion of genes encoding either the receptor or a single agonist, this in turn may subtly alter the immunological status of the mice and lead to a profound phenotype under inflammatory conditions, (2) antibody neutralization of one or two agonists; however, this strategy only partly blocks the CXCR3 signalling axis (Fife *et al*., 2001; Hildebrandt *et al*., 2004), (3) the use of a polyclonal anti-CXCR3 antibody, which may have promoted cell depletion (Xie *et al*., 2003) and (4) small molecule antagonists, these may be limited by PK properties such as short half-life and area under the curve. The PK/PD format of the CXCR3 receptor internalization assay described in this study enabled us to determine that a once daily subcutaneous administration of the small molecule CXCR3 antagonist NBI-74330 would provide approximately 82% CXCR3 occupancy. Based on this PK/PD readout, this dosing regimen may be the most appropriate to establish the pharmacological tractability of this target in murine models of chronic inflammatory disease.

This finding demonstrates the utility of the CXCR3 receptor internalization assay to discriminate between dosing regimens and enable the evaluation of the role of CXCR3 in murine models of chronic inflammatory disease. We believe that these types of studies are essential to underpin target validation experiments in more complex models of inflammation.

Acknowledgements

We gratefully acknowledge the technical assistance of Paul Green for conducting PK experiments, Kevin Minton for conducting the antibody–agonist competition studies and Bob Watson for synthesis of NBI-74330 and metabolite-1. We are also extremely grateful to Gayle Chapman for helpful discussions.

Conflict of interest

The authors state no conflict of interest.

References

Arai H, Monteclaro FS, Tsou CL, Franci C, Charo IF (1997). Dissociation of chemotaxis from agonist-induced receptor internalization in a lymphocyte cell line transfected with CCR2B. Evidence that directed migration does not require rapid modulation of signaling at the receptor level. *J Biol Chem* **272**: 25037–25042.

Blue Jr DR, Bonhaus DW, Ford AP, Pfister JR, Sharif NA, Shieh IA *et al*. (1995). Functional evidence equating the pharmacologically-defined alpha 1A- and cloned alpha 1C-adrenoceptor: studies in the isolated perfused kidney of rat. *Br J Pharmacol* **115**: 283–294.

Bonecchi R, Bianchi G, Bordignon PP, D'Ambrosio D, Lang R, Borsatti A *et al*. (1998). Differential expression of chemokine receptors and chemotactic responsiveness of type 1 T helper cells (Th1s) and Th2s. *J Exp Med* **187**: 129–134.

Campanella GS, Lee EM, Sun J, Luster AD (2003). CXCR3 and heparin binding sites of the chemokine IP-10 (CXCL10). *J Biol Chem* **278**: 17066–17074.

Campbell DB (1990). The use of kinetic–dynamic interactions in the evaluation of drugs. *Psychopharmacology (Berl)* **100**: 433–450.

Christensen JE, de Lemos C, Moos T, Christensen JP, Thomsen AR (2006). CXCL10 is the key ligand for CXCR3 on CD8+ effector T cells involved in immune surveillance of the lymphocytic choriomeningitis virus-infected central nervous system. *J Immunol* **176**: 4235–4243.

Christensen JE, Nansen A, Moos T, Lu B, Gerard C, Christensen JP *et al*. (2004). Efficient T-cell surveillance of the CNS requires expression of the CXC chemokine receptor 3. *J Neurosci* **24**: 4849–4858.

Clark-Lewis I, Mattioli I, Gong JH, Loetscher P (2003). Structure–function relationship between the human chemokine receptor CXCR3 and its ligands. *J Biol Chem* **278**: 289–295.

Colburn WA (2000). Optimizing the use of biomarkers, surrogate endpoints, and clinical endpoints for more efficient drug development. *J Clin Pharmacol* **40**: 1419–1427.

Colvin RA, Campanella GS, Sun J, Luster AD (2004). Intracellular domains of CXCR3 that mediate CXCL9, CXCL10, and CXCL11 function. *J Biol Chem* **279**: 30219–30227.

Dorland RB, Middlebrook JL, Leppla SH (1979). Receptor-mediated internalization and degradation of diphtheria toxin by monkey kidney cells. *J Biol Chem* **254**: 11337–11342.

Eriksson C, Eneslatt K, Ivanoff J, Rantapaa-Dahlqvist S, Sundqvist KG (2003). Abnormal expression of chemokine receptors on T-cells from patients with systemic lupus erythematosus. *Lupus* **12**: 766–774.

Fife BT, Kennedy KJ, Paniagua MC, Lukacs NW, Kunkel SL, Luster AD *et al*. (2001). CXCL10 (IFN-gamma-inducible protein-10) control of encephalitogenic CD4+ T cell accumulation in the central nervous system during experimental autoimmune encephalomyelitis. *J Immunol* **166**: 7617–7624.

Forster R, Kremmer E, Schubel A, Breitfeld D, Kleinschmidt A, Nerl C *et al*. (1998). Intracellular and surface expression of the HIV-1 coreceptor CXCR4/fusin on various leukocyte subsets: rapid internalization and recycling upon activation. *J Immunol* **160**: 1522–1531.

Furchgott R (1966). The use of β-haloalkylamines in the differentiation of receptors and in the determination of dissociation constants of receptor-agonist complexes. In: Harper J, Simmonds AB (eds). Advances in drug research, vol. 3. Academic Press: New York, pp 21–55.

Gaddum JH, Hameed KA, Hathway DE, Stephens FF (1955). Quantitative studies of antagonists for 5-hydroxytryptamine. *Q J Exp Physiol Cogn Med Sci* **40**: 49–74.

Gao P, Zhou XY, Yashiro-Ohtani Y, Yang YF, Sugimoto N, Ono S *et al*. (2003). The unique target specificity of a nonpeptide chemokine receptor antagonist: selective blockade of two Th1 chemokine receptors CCR5 and CXCR3. *J Leuk Biol* **73**: 273–280.

Gonsiorek W, Zavodny P, Hipkin RW (2003). The study of CXCR3 and CCR7 pharmacology using [^{35}S]GTPgammaS exchange assays in cell membranes and permeabilized peripheral blood lymphocytes. *J Immunol Methods* **273**: 15–27.

Hancock WW, Gao W, Csizmadia V, Faia KL, Shemmeri N, Luster AD (2001). Donor-derived IP-10 initiates development of acute allograft rejection. *J Exp Med* **193**: 975–980.

Hancock WW, Lu B, Gao W, Csizmadia V, Faia K, King JA *et al*. (2000). Requirement of the chemokine receptor CXCR3 for acute allograft rejection. *J Exp Med* **192**: 1515–1520.

Heise CE, Pahuja A, Hudson SC, Mistry MS, Putnam AL, Gross MM *et al*. (2005). Pharmacological characterization of CXC chemokine receptor 3 ligands and a small molecule antagonist. *J Pharmacol Exp Ther* **313**: 1263–1271.

Hildebrandt GC, Corrion LA, Olkiewicz KM, Lu B, Lowler K, Duffner UA *et al*. (2004). Blockade of CXCR3 receptor:ligand interactions reduces leukocyte recruitment to the lung and the severity of experimental idiopathic pneumonia syndrome. *J Immunol* **173**: 2050–2059.

Hsieh MF, Lai SL, Chen JP, Sung JM, Lin YL, Wu-Hsieh BA *et al*. (2006). Both CXCR3 and CXCL10/IFN-inducible protein 10 are required for resistance to primary infection by dengue virus. *J Immunol* **177**: 1855–1863.

Jenkinson DH (1991). How we describe competitive antagonists: three questions of usage. *Trends Pharmacol Sci* **12**: 53–54.

Jiang D, Liang J, Hodge J, Lu B, Zhu Z, Yu S *et al*. (2004). Regulation of pulmonary fibrosis by chemokine receptor CXCR3. *J Clin Invest* **114**: 291–299.

Kaumann AJ, Frenken M (1985). A paradox: the 5-HT2-receptor antagonist ketanserin restores the 5-HT-induced contraction depressed by methysergide in large coronary arteries of calf. Allosteric regulation of 5-HT2-receptors. *Naunyn Schmiedebergs Arch Pharmacol* **328**: 295–300.

Kaumann AJ, Frenken M (1988). ICI 169369 is both a competitive antagonist and an allosteric activator of the arterial 5-hydroxytryptamine2 receptor system. *J Pharmacol Exp Ther* **245**: 1010–1015.

Koenig JA, Edwardson JM (1997). Endocytosis and recycling of G protein-coupled receptors. *Trends Pharmacol Sci* **18**: 276–287.

Liu YJ, Shankley NP, Welsh NJ, Black JW (1992). Evidence that the apparent complexity of receptor antagonism by angiotensin II analogues is due to a reversible and syntopic action. *Br J Pharmacol* **106**: 233–241.

Loetscher M, Gerber B, Loetscher P, Jones SA, Piali L, Clark-Lewis I *et al*. (1996). Chemokine receptor specific for IP10 and mig: structure, function, and expression in activated T-lymphocytes. *J Exp Med* **184**: 963–969.

Loetscher M, Loetscher P, Brass N, Meese E, Moser B (1998). Lymphocyte-specific chemokine receptor CXCR3: regulation, chemokine binding and gene localization. *Eur J Immunol* **28**: 3696–3705.

Marchese A, Heiber M, Nguyen T, Heng HH, Saldivia VR, Cheng R *et al*. (1995). Cloning and chromosomal mapping of three novel genes, GPR9, GPR10, and GPR14, encoding receptors related to interleukin 8, neuropeptide Y, and somatostatin receptors. *Genomics* **29**: 335–344.

Medina JC, Johnson MG, TularikInc. (2002). CXCR3 antagonists WO02083143.

Monteclaro FS, Charo IF (1997). The amino-terminal domain of CCR2 is both necessary and sufficient for high affinity binding of monocyte chemoattractant protein 1. Receptor activation by a pseudo-tethered ligand. *J Biol Chem* **272**: 23186–23190.

Overington JP, Al Lazikani B, Hopkins AL (2006). How many drug targets are there? *Nat Rev Drug Discov* **5**: 993–996.

Paton WD, Rang HP (1965). The uptake of atropine and related drugs by intestinal smooth muscle of the guinea-pig in relation to acetylcholine receptors. *Proc R Soc Lond B Biol Sci* **163**: 1–44.

Pease JE, Williams TJ (2006). The attraction of chemokines as a target for specific anti-inflammatory therapy. *Br J Pharmacol* **147** (Suppl 1): S212–S221.

Pendleton RG, Gessner G, Horner E (1989). Studies on inhibition of angiotensin II receptors in rabbit adrenal and aorta. *J Pharmacol Exp Ther* **248**: 637–643.

Proost P, Schutyser E, Menten P, Struyf S, Wuyts A, Opdenakker G *et al*. (2001). Amino-terminal truncation of CXCR3 agonists impairs receptor signaling and lymphocyte chemotaxis, while preserving antiangiogenic properties. *Blood* **98**: 3554–3561.

Rabin RL, Park MK, Liao F, Swofford R, Stephany D, Farber JM (1999). Chemokine receptor responses on T cells are achieved through regulation of both receptor expression and signaling. *J Immunol* **162**: 3840–3850.

Robertson MJ, Dougall IG, Harper D, McKechnie KC, Leff P (1994). Agonist–antagonist interactions at angiotensin receptors: application of a two-state receptor model. *Trends Pharmacol Sci* **15**: 364–369.

Sallusto F, Lenig D, Mackay CR, Lanzavecchia A (1998). Flexible programs of chemokine receptor expression on human polarized T helper 1 and 2 lymphocytes. *J Exp Med* **187**: 875–883.

Sauty A, Colvin RA, Wagner L, Rochat S, Spertini F, Luster AD (2001). CXCR3 internalization following T cell–endothelial cell contact: preferential role of IFN-inducible T cell alpha chemoattractant (CXCL11). *J Immunol* **167**: 7084–7093.

Sauty A, Dziejman M, Taha RA, Iarossi AS, Neote K, Garcia-Zepeda EA *et al*. (1999). The T cell-specific CXC chemokines IP-10, Mig, and I-TAC are expressed by activated human bronchial epithelial cells. *J Immunol* **162**: 3549–3558.

Schild HO (1949). pA_x and competitive drug antagonism. *Br J Pharmacol* **4**: 277–280.

Schneller SW, Luo JK (1980). Synthesis of 4-amino-lH-pyrrolo[2,3-b] pyridine (1,7-dideazaadenine) and lH-pyrrolo[2,3-b]pyridin-4-ol (1,7-dideazahypoxanthine). *J Org Chem* **45**: 4045–4048.

Sorensen TL, Tani M, Jensen J, Pierce V, Lucchinetti C, Folcik VA *et al*. (1999). Expression of specific chemokines and chemokine receptors in the central nervous system of multiple sclerosis patients. *J Clin Invest* **103**: 807–815.

Tensen CP, Flier J, van der Raaij-Helmer EM, Sampat-Sardjoepersad S, van der Schors RC, Leurs R *et al*. (1999). Human IP-9: a keratinocyte-derived high affinity CXC-chemokine ligand for the IP-10/Mig receptor (CXCR3). *J Invest Dermatol* **112**: 716–722.

Walker DK (2004). The use of pharmacokinetic and pharmacodynamic data in the assessment of drug safety in early drug development. *Br J Clin Pharmacol* **58**: 601–608.

Xanthou G, Williams TJ, Pease JE (2003). Molecular characterization of the chemokine receptor CXCR3: evidence for the involvement of distinct extracellular domains in a multi-step model of ligand binding and receptor activation. *Eur J Immunol* **33**: 2927–2936.

Xie JH, Nomura N, Lu M, Chen SL, Koch GE, Weng Y *et al*. (2003). Antibody-mediated blockade of the CXCR3 chemokine receptor results in diminished recruitment of T helper 1 cells into sites of inflammation. *J Leuk Biol* **73**: 771–780.